

Multiaxial Stress in the Fatigue Life of Mechanical Parts

Ademar de Azevedo Cardoso

GAC Soluções

Silvio Castro Alano

Altair Engineering do Brasil

Copyright © 2011 SAE International

ABSTRACT

Approximated analytical methods for evaluation notch stress and strain under multiaxial loading are considered. Results from analytical methods are compared to results from elastic-plastic finite element analysis. An engine bearing cap is evaluated under both methods, considering the services load from the combustion pressure and also the bolt tension. Linear kinematic hardening rule and Mises plasticity model have been considered. Results from analytical models and nonlinear finite element analysis are compared.

INTRODUCTION

Finding out stress and strain at notch areas is a mandatory step in the design of most mechanical components. From the fatigue analysis point of view, notches regions are often the preferred sites for crack initiation. If the component is subjected to variable loading, plastic deformation in the notch area can significantly decrease the durability of the component, often with undesirable failures. Besides, notch fatigue behavior is usually better represented by strain based approach, which demands the knowledge of notch of stress and strain magnitudes.

Notches are found in most engineering structural components. Structural discontinuities such as shoulders, holes, fillets, grooves and keyways, are example of notches. In the notch, stress increases due to several reasons, e.g., complex geometrical details, defects in the fabrication process or failures in the assembling procedure.

The amplification in the stress magnitude can be measured by the stress concentration factor (K_t), which relates the notch root stress to the nominal stress. The material's elastic behavior also allows writing K_t as the ratio of notch root strain to the nominal strain. In a mathematical form one can state

$$K_t = \frac{\sigma}{S} = \frac{\varepsilon}{e} \quad (1.a)$$

given that $\sigma/\varepsilon=E=\text{constant}$. (1.b)

For simple geometries, stress concentration factor for elastic materials can be measured by analytical^{1,2}, experimental³⁻⁵ and numerical methods, as the finite element linear analysis⁶⁻¹⁰. The later approach, however, is the common method used for K_t calculation of complex geometries and general load cases.

If notch stress is higher than the material yield stress, Hooke's law can not relate the notch stress (σ) to the notch strain (ε). Consequently, both local strain and local stress no longer can be related to nominal stress and strain, respectively. Beyond the yield stress, notch stress and strain can be related to the relate to the respective nominal values by the stress and strain concentration factors (K_σ and K_ε , respectively), defined by

$$K_\sigma = \frac{\sigma}{S} \text{ and } K_\varepsilon = \frac{\varepsilon}{e} \quad (2)$$

The elastic-plastic behavior of many materials can be obtained by experimental strain gage. Common engineering materials show stress-strain behavior that can be modeled by Ramberg-Osgood equation, as follows

$$\varepsilon = \frac{\sigma}{E} + \left(\frac{\sigma}{H} \right)^{1/n} \quad (3)$$

where:

H is the monotonic cyclic strength and

n is the monotonic cyclic exponent.

For each material, the parameters H and n are adjusted to fit experimental results.

If elastic-plastic finite element analysis is used for evaluated stress and strain of yielded components, small element size in the high-stress gradient regions is required for solution accuracy. Besides, a realistic representation of the nonlinear material stress-strain behavior is required¹¹.

Additionally, for a cyclic elastic-plastic analysis, a cyclic plasticity model is required. The cyclic model should be composed of three major components¹²:

- (a) a *yield function*, to describe the combinations of stress that will lead to plastic flow
- (b) a *flow rule*, to describe the relationship between the stresses and plastic strains during plastic deformation and
- (c) a *hardening rule*, to describe how the yield criterion changes with plastic straining.

Although nonlinear finite element analysis can be used as an accurate tool for evaluating the cyclic notch stress-strain behavior, it is often a time-consuming and expensive method, particularly for long service load histories. For this reason, analytical methods that estimate the notch stress and strain are commonly used in fatigue design of components.

The elastic stress concentration factor (K_t) required by analytical methods, can be obtained by linear finite element, specially for complex geometries. In this way, a combination of analytical methods and linear finite element analysis provides notch stress and strain.

Perhaps the most widely used procedure for estimating notch strain in the plastic region is Neuber's rule or equivalent approaches based on strain energy¹². Several modifications of these rules¹⁴⁻²⁵ have been derived in the last decades. Particularly, modifications proposed by Dowling¹⁴ and Hoffmann and Seeger¹⁵ are addressed for dealing with proportional multiaxial stress.

In this paper, fatigue life estimation of bearing cap subject to services loading is evaluated. Notch stress and strain on the bearing cap are calculated by nonlinear elastic-plastic finite element analysis. The numerical results are compared with results from analytical methods proposed by Dowling and Hoofmnan and Seeger. Results of analytical model are compared to elastic-plastic analysis results of the component for monotonic loading.

After calculating notch stress and strain, the strain life approach is employed for fatigue estimation. Bolt tension and combustion pressure load lead to a multiaxial stress states in the relevant notch areas of the bearing cap.

NEUBER'S RULE

Neuber²⁶ derived the theory for approximating notch stress concentration of a prismatic beam subjected to pure shear loading. Neuber's rule states that the geometrical mean of stress and strain concentration factors remains constant during plastic deformation.

$$K_t^2 = K_\sigma K_\epsilon \quad (4)$$

Neuber's rule overestimates the notch strain for typical plane strain components and provides good results for thin shell and plates parts²³.

For elastic nominal stress, Equations (1), (2) and (4) are combined to give

$$\sigma \cdot \epsilon = \frac{(K_t S)^2}{E} \quad (5)$$

Notch stress (σ) and strain (ϵ) can be obtained by simultaneous solution of Equations 3 and 5, what can be done by graphical or numerical methods. Linear finite element analysis furnish the squared term on the right side of Equation 5.

MULTIAXIAL GENERALIZATION OF NEUBER'S RULE

Under proportional loads, multiaxial stress and strain at notch roots can be treated by several proposed extensions of Neuber's rule^{14,15,18,21}. Using the von Mises flow criterion to calculate equivalent stress, Neuber's rules can be stated as

$${}^e \sigma^{eq} \cdot {}^e \epsilon^{eq} = \sigma^{eq} \cdot \epsilon^{eq} \quad (6)$$

Solutions of Equation 6 for proportional loads usually consider that ratios of principal stresses and/or ratio of principal strain remain constant during plastic deformation. Since Poisson ratio is not constant, such assumption provides acceptable results for small plastic deformation.

Dowling's approximation performs a multiaxial notch analysis by changing the material properties. The modulus of elasticity (E) and Ramberg-Osgood's strength coefficient (H) are modified by the assumption that stress normal to the free surface is zero and also that principal strain ratio θ_2 and principal stress ratio λ_2 remain constant, viz.

$$\theta_2 = \frac{\epsilon_2}{\epsilon_1} \approx \frac{{}^e \epsilon_2}{{}^e \epsilon_1} \quad (7)$$

$$\lambda_2 = \frac{\sigma_2}{\sigma_1} \approx \frac{{}^e \sigma_2}{{}^e \sigma_1} \quad (8)$$

So, the effective material properties can be written as

$$E^* = E \cdot \frac{(1 + \nu \cdot \theta_2)}{(1 - \nu^2)} \quad (9)$$

and

$$H^* = H \cdot \left(\frac{2}{2 - \lambda_2} \right)^n (\lambda_2^2 - \lambda_2 + 1)^{\frac{n-1}{2}} \quad (10)$$

Neuber's rule can be written in terms of the major principal stress and strain as¹²

$$\frac{e \sigma_{eq}^2}{E} = \sigma_1 \cdot \varepsilon_1 = \frac{\sigma_1^2}{E^*} + \sigma_1 \cdot \left(\frac{\sigma_1}{H^*} \right)^{1/n} \quad (11)$$

where

$$e \sigma_{eq} = \sqrt{e \sigma_1^2 + e \sigma_2^2 - e \sigma_1^2 \cdot e \sigma_2^2} \quad (12)$$

is the equivalent von Mises stress for elastic analysis.

Equations 11 are resolved in σ_1 and ε_1 , as long as $e \sigma_{eq}$ is delivered by linear results of finite element analysis.

After calculating σ_1 and ε_1 , the second principal stress, σ_2 , and strain, ε_2 , can be calculated by Equations 7–8, respectively.

The normal surface deformation's, ε_3 , is calculated by

$$\varepsilon_3 = -\bar{\nu} \cdot \frac{1 + \lambda}{1 - \bar{\nu} \cdot \lambda} \cdot \varepsilon_1 \quad (13)$$

where

$$\bar{\nu} = \frac{1}{2} - \left(\frac{1}{2} - \nu \right) \frac{\sigma_1}{E^* \cdot \varepsilon_1} \quad (14)$$

Hoffmann and Seeger¹⁵ also considered that the stress (σ_3) normal to the surface is zero. For nominal elastic strain under proportional load, they proposed that Neuber's rule can be written by

$$\frac{e \sigma_{eq}^2}{E} = \sigma_{eq} \cdot \varepsilon_{eq} = \frac{\sigma_{eq}^2}{E} + \sigma_{eq} \cdot \left(\frac{\sigma_{eq}}{H} \right)^{1/n} \quad (15)$$

Equations 15 can be resolved in σ_{eq} and ε_{eq} , where $e \sigma_{eq}$ is calculated by Equation 12.

Considering that principal strain ratio θ_2 remains constant during the plastic deformation, Equations 16-20 can be resolved in σ_1 , σ_2 , ε_1 , ε_2 and ε_3 .

$$\varepsilon_1 = \frac{\varepsilon_{eq}}{\sigma_{eq}} \cdot (\sigma_1 - \bar{\nu} \sigma_2) \quad (16)$$

$$\varepsilon_2 = \frac{\varepsilon_{eq}}{\sigma_{eq}} \cdot (-\bar{\nu} \sigma_1 + \sigma_2) \quad (17)$$

$$\varepsilon_3 = \frac{\varepsilon_{eq}}{\sigma_{eq}} \cdot (-\bar{\nu} (\sigma_1 + \sigma_2)) \quad (18)$$

$$\sigma_1 = \frac{1}{\sqrt{1 - \bar{\lambda}_2 + \bar{\lambda}_2^2}} \cdot \sigma_{eq} \quad (19)$$

$$\varepsilon_1 = \frac{1}{\sqrt{1 - \bar{\lambda}_2 + \bar{\lambda}_2^2}} \cdot \varepsilon_{eq} \quad (20)$$

where

$$\bar{\nu} = \frac{1}{2} - \left(\frac{1}{2} - \nu \right) \frac{\sigma_{eq}}{E \cdot \varepsilon_{eq}} \quad (21)$$

and

$$\bar{\lambda}_2 = \frac{\bar{\nu} + \theta_2}{1 + \bar{\nu} \cdot \theta_2} \quad (22)$$

FEM ANALYSIS

Elastic-plastic analysis was performed using the FEM package RADIOSS²⁵ program. The linear kinematic plastic rule and the Mises yield function have been considered in the nonlinear analysis.

The material's monotonic properties are shown in Table 1 and the stress-strain curve is sketched in Figure 1.

Table 1 – Material properties of bearing cap.

Tensile Strength (Su)	850 MPa
Yield Strength (Sy)	395 MPa
Modulus of Elasticity (E)	210 GPa
Poisson's Ratio (u)	0.3
Fatigue Strength (Se)	200 MPa
Monotonic strength coefficient (H)	1400 MPa
Monotonic strength exponent (n)	0.122
Fatigue ductility coefficient (ε'_f)	0.31
Fatigue ductility exponent (c)	-0.621
Fatigue strength coefficient (σ'_f)	1350
Fatigue strength exponent (b)	-0.0758

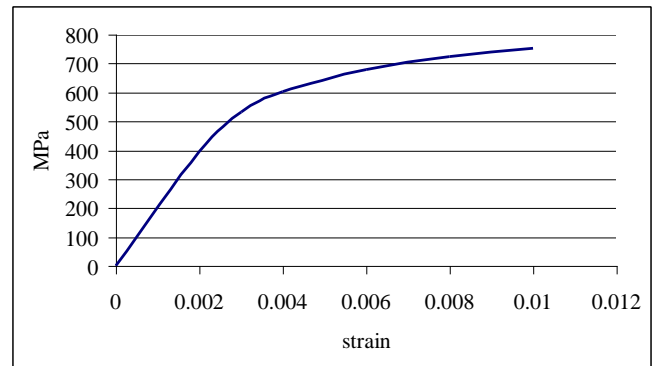


Figure 1 – Stress-strain curve for bearing cap analysis.

As shown in Figures 2–5, geometrical shape of bearing cap has been modeled by using parabolic tetra elements. Only a quarter of the bearing cup has modeled due to symmetries of load and geometry.

Bolt is modeled by beam and rigid elements. Beam element is used to represent the length of the bolt. Rigid elements provide the connection between beam and tetra solid elements. Such connection is performed by considering the approximated area of contact of the bolt head with the bearing cap.

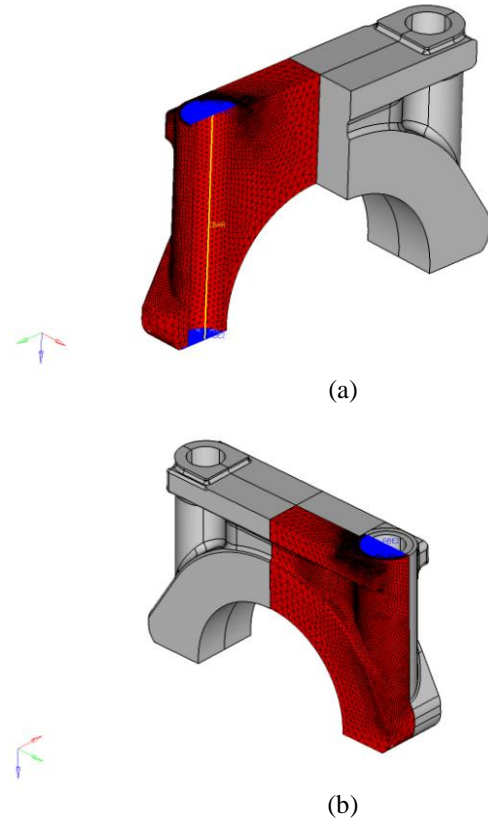


Figure 2 – Geometry and a quarter FE model for bearing cap.

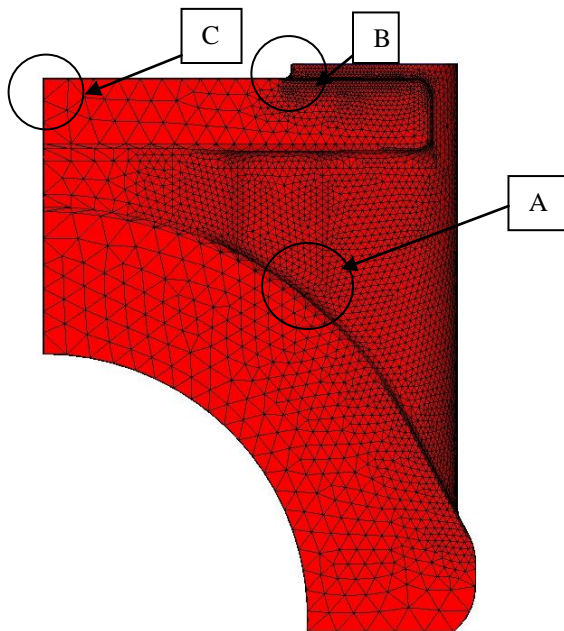


Figure 3 – FE model for bearing cap analysis.

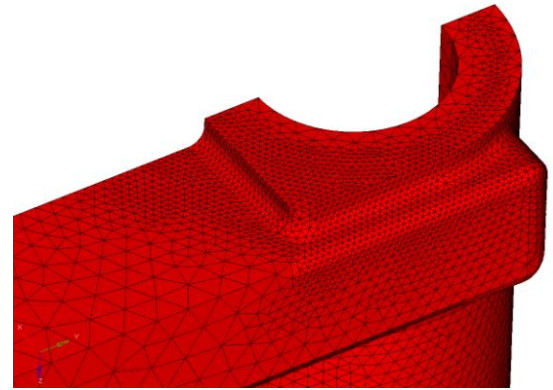


Figure 4 – FE meshing detail on region B.

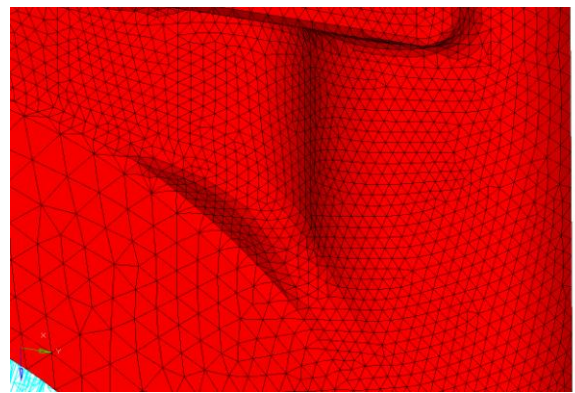


Figure 5 – FE meshing detail on region A.

Meshing size was refined in the interested regions, as shown in Figure 3–5. In those regions, identified as areas A and B in Figure 3, typical element size is 0.5 mm. The area C has also been evaluated.

The mesh refinement has been considered until get acceptable difference between averaged and unaveraged maximum principal stress on the notch areas (less than 5%).

FE model has been first loaded with an axial force resulting from torque on the bearing cap bolt. Next, forces from combustion pressure transmitted by the crankshaft were considered, as illustrated in Figure 6. The pressure distribution is considered by a cosine function, with maximum value at the center of the cap, going to zero at the lateral.

Load from combustion pressure has been increase to produce plastic strain in the bearing cap. The nominal values have been accordingly multiplied by 1.3, 1.6 e 2.0 to get the points for comparison in the plastic region of stress-strain curve.

RESULTS

The comparison of the three different approach has been done in terms of notch equivalent stress. Nevertheless, similar conclusions can be taken from comparison of the principal stresses. As nonlinear and linear analysis have been performed on the same meshing, the comparison could be done at each node.

Results from nonlinear FEM analysis have been obtained directly from the post-processing of each load case: the principal stresses were acquired to evaluate Equation 12 (without the upper e) and also the principal strains were obtained to be applied in Equation 22.

Hoofmann-Seeger and Dowling expressions have been performed from the results of FEM linear static analysis. Equations 11 and 15 have been resolved in $\sigma_I - \varepsilon_I$ and $\sigma_{eq} - \varepsilon_{eq}$, respectively, by iterative numerical procedure.

To exemplify the analyses, results for worst node in area B are shown in Table 2.

Table 2 – FEM Linear Stresses and Strains.

load factor	$^e\varepsilon_1$	$^e\varepsilon_2$	$^e\sigma_1(\text{MPa})$	$^e\sigma_2(\text{MPa})$
1.0	1.458E-03	-5.724E-04	297.7	-27.7
1.3	2.033E-03	-7.515E-04	418.0	-28.2
1.6	2.603E-03	-9.301E-04	537.4	-29.0
2.0	3.373E-03	-1.172E-03	698.3	-30.2

After solving for each load, the notch equivalent stress for both expressions has been evaluated, as given in Table 3.

Table 3 – Notch Equivalent Stress and Strains.

area B	Notch Equivalent Stress (MPa)		
strain ($\mu\varepsilon$)	FEM	Seeger	Dowling
1394.5	300.4	312.0	322.3
1919.3	428.9	426.9	435.9
2440.1	447.9	522.3	528.9
3143.6	619.3	610.7	614.8

Typical stress distributions are depicted in Figures 8–9. In Figure 9, maximum principal stress on the area B is shown.

Comparative results obtained are depicted in Figures 10–12. The graphics are plotted with nominal micro-strain in the longitudinal axis and the notch stress in the vertical axis.

In Figure 11 is shown the maximum notch stress in the area B. The values obtained from Dowling and Hoffman-Seeger analytical methods are close related. The maximum difference to FEM results is 10%.

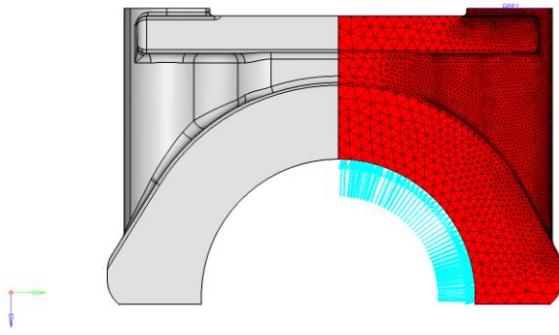


Figure 6 – Pressure on the cap from cylinder fire.

In Figure 7 is shown the symmetric planes where boundary conditions have been applied. The bearing cap's surface that contacts the engine block has also been clamped.

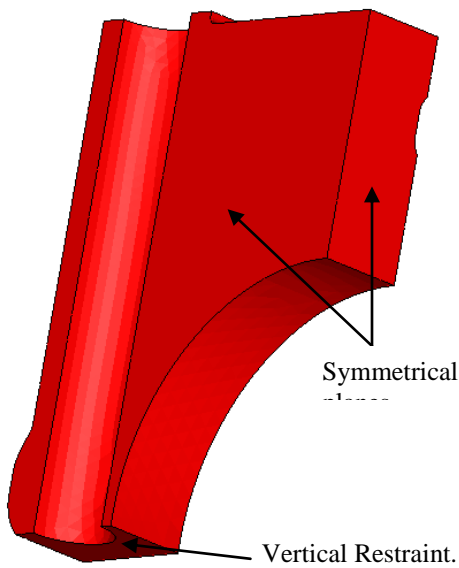


Figure 7 – FE boundary conditions.

FATIGUE ANALYSIS

The strain-based approach to life estimation of the bearing cap has been calculated by Morrow's equation, including the effects of the mean stress, given by¹¹

$$\varepsilon_a = \frac{\sigma'_f - \sigma_m}{E} (2N_f)^b + \varepsilon'_f (2N_f)^c \quad (22)$$

Where

ε_a – total strain amplitude.

ε'_f – fatigue ductility coefficient.

c – fatigue ductility exponent.

σ'_f – fatigue strength coefficient.

σ_f – fatigue strength coefficient.

σ_m – mean stress.

b – fatigue strength exponent.

$2N_f$ – number de reversals to failure.

Similar results can be observed from Figures 11 and 12. In both cases, there is a variation in the FEM results for the third point plot. The FEM model has been revised and no consistent reason was found for such behavior. The maximum difference to FEM results is 16% in the area A, and 18% in the area C.

Areas with compressive principal stresses also have been focused. However, we had some difficulties to obtain results with Dowling approach. In the points analyzed, the effective strength coefficient (H) decreases significantly, also affecting the effective Poisson ratio. As fatigue problems are concerned to tensile areas, compressive areas were not considered.

Fatigue life of bearing cap has been estimated considering a majority factor of 30% over the nominal load. The cyclic load is between (a) only bolt loading to (b) bolt load plus the force from combustion pressure.

Considering Equation 22 and the fatigue parameters shown in Table 1, infinite life has been obtained for area B of the bearing cap.

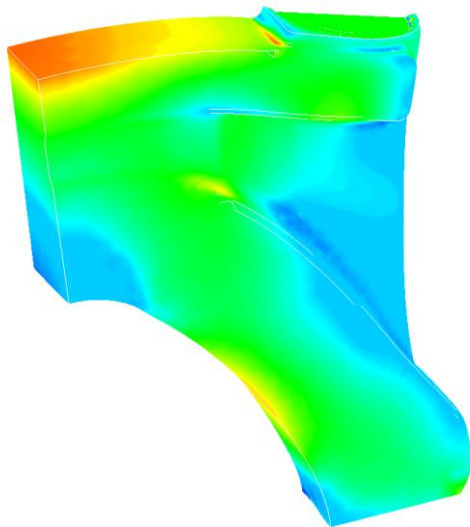


Figure 8 – Maximum principal stress distribution in the bearing cap.

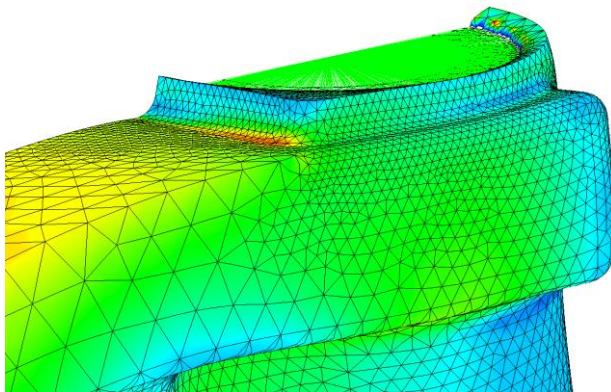


Figure 9 – Typical stress distribution in notch area B.

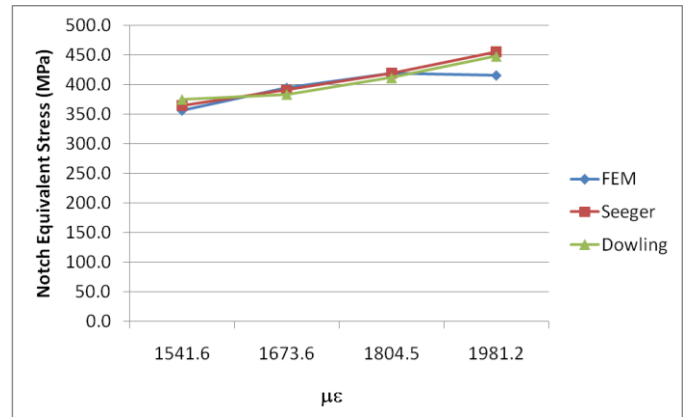


Figure 10 – Notch stress vs. nominal strain – Area A.

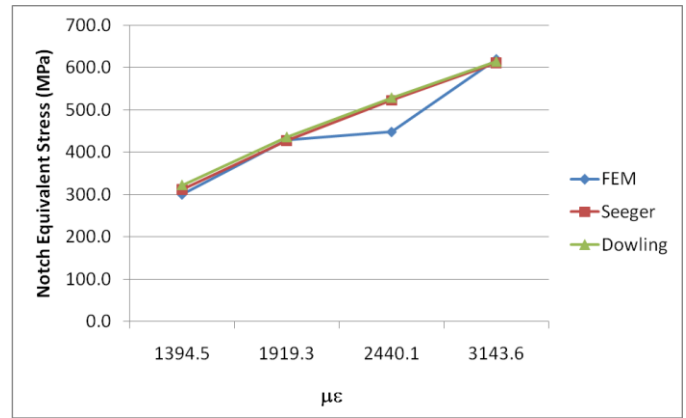


Figure 11 – Notch stress vs. nominal strain – Area B.

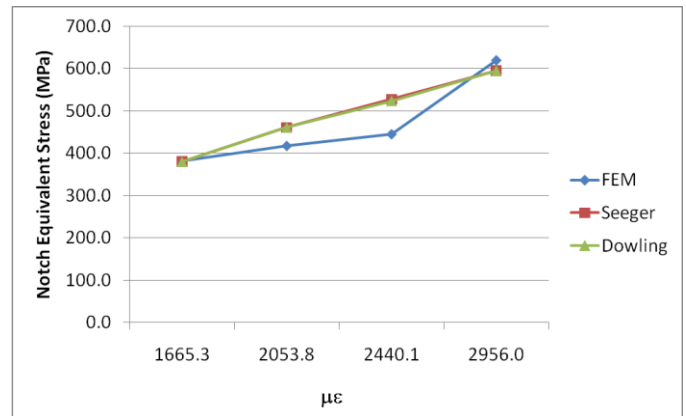


Figure 12 – Notch stress vs. nominal strain – Area C.

CONCLUSIONS

The bearing cap has been evaluated for two analytical methods and for nonlinear finite element analysis. Results observed from both Dowling and Hoffmann–Seeger methods are encouraged. With notch stress and strain calculated, several strain life equation can be employed to calculate fatigue life.

It is worth to note that the good agreement of models which consider constant ratios for principal stress and/or strain are close related to small plastic deformation²⁶. If the yielding is achieved in a large area, results from closed form expressions, like (11) and (15), move away from nonlinear analysis results.

This study shows that it is possible to get accurate plastic stress and strain results using linear FEM analysis implementing a correction plastic rule. For fatigue analysis these models can also be implemented during the cycles counting, resulting in a faster analysis computation.

REFERENCES

- Pilkey, W.D., *Peterson's Stress Concentration Factors*, J.Wiley & Sons, New York, 1997.
- Young, W.C.; Budynas, R.G. *Roarks's formulas for stress and strain*, McGraw-Hill, New York, 2002.
- Loqman, Ahmad, et alii, *An Experimental Investigation of Stress Concentration Factor*, Nanyang Technological University, Nanyang, 2000.
- Gerdeen, J. C., Smith, R.E., *Experimental determination of stress-concentration factors in thick-walled cylinders with crossholes and side holes*, *Experimental Mechanics*, Vol.12, p.530, 1972
- Issa, S.S., Maamoun, G. A., *Novel Photoelastic Approach in Analysis of Elliptical Holes in Thick Plates*, *Journal of Engineering Mechanics*, Vol. 118, p. 1631, 1992.
- Garrell, M.G., et alii, *Finite-Element Analysis of Stress Concentration in ASTM D 638 Tension Specimens*, *Journal of Testing and Evaluation*, Vol.31, p.1, 2003.
- Paul, T. K., Rao, K. M., *Finite element evaluation of stress concentration factor of thick laminated plates under transverse loading*, *Computers & Structures*, Vol. 48, p. 311, 1993.
- Efthymoiu, M., Durkin, S., *Stress concentration in T/Y and gap/overlap K-joints*, *Proceedings of 4th International Conference on Behavior of Offshore Structures*, Delft, 1985.
- Kuang, J.G., et alii, *Stress concentration in tubular joints*, *Proceedings of 7th Offshore Technology Conference*, Houston, 1975.
- Cardoso, A.A., Augusto, O.B, Dias, C.A.N., *Considerations on artificial neural networks in the stress concentration factor for tubular joints*, *Proceedings of 17th International Conference on Offshore Mechanics and Arctic Engineering*, Lisboa, 1998.
- Stephens, R.I., et alii, *Metal Fatigue in Engineering*, 2nd ed., Wiley, New York, 2001.
- Socie, D.F., Marquis, G.B., *Multiaxial Fatigue*, Society of Automotive Engineers, Warrendale, 1999.
- Neuber H. *Theory of stress concentration for shear-strained prismatic bodies with arbitrary nonlinear stress-strain law*. *Journal of Applied Mechanics*, Vol.28, p.544, 1961.
- Dowling, N.E., Brose, W.R. & Wilson, W.K., *Notched member fatigue life predictions by the local strain approach*. *Fatigue Under Complex Loading: Analysis and Experiments*, AE-6, SAE, 1977.
- Hoffmann, M., Seeger, T., *A generalized method for estimating multiaxial elastic-plastic notch stresses and strains. Part I: Theory*. *Journal of Engineering Materials and Technology* Vol. 107, p.250, 1985.
- Glinka, G., *Calculation of inelastic notch-tip strain-stress histories under cyclic loading*. *Engineering Fracture Mechanics*. Vol. 22, p.839, 1985.
- Ye, D., et alii, *Further investigation of Neuber's rule and the equivalent strain energy density (ESED) method*, *International Journal of Fatigue*, Vol.26, p.447, 2004.
- Ye, D., Hertel, O., Vormwald, M., *A unified expression of elastic-plastic notch stress-strain calculation in bodies subjected to multiaxial cyclic loading*, *International Journal of Solids and Structures*, Vol. 45, p. 6177, 2008.
- Adibi-Asl, R., Seshadri, R. *Improved Prediction Method for Estimating Notch Elastic-Plastic Strains*, 19th International Conference on Structural Mechanics in Reactor Technology, Toronto, 2007.
- Lim, J.Y., Hong, S.G., Lee, S.B., *Application of local stress-strain approaches in the prediction of fatigue crack initiation life for cyclically non-stabilized and non-Masing steel*, *International Journal of Fatigue*, Vol. 27, p. 1653, 2005.
- Sethuraman, R., Gupta, S.V., *Evaluation of notch root elasto-plastic stress-strain state for general loadings using an elastic solution*, *International Journal of Pressure Vessels and Piping*, Vol 81, p.313, 2004.
- Yip, M.C., Jen, Y.M., *Biaxial fatigue crack initiation life prediction of solid cylindrical specimens with transverse circular holes*, *International Journal of Fatigue*, Vol. 18, No. 2, p. 111, 1996
- Fatemi, A., Fang, D., Zeng, Z., *Notched Fatigue Behavior Under Axial and Torsion Loads: Experiments and Predictions*, 8th International Fatigue Congress, Vol.3, p.1905, Stockholm, 2002.
- Fatemi, A., Zeng, Z., *Elasto-plastic stress and strain behavior at notch roots under monotonic and cyclic loadings*, *Journal of Strain Analysis*, Vol 36, pg 287, 2001.
- Altair Engineering RADIOSS 11.0 – Users Guide, Troy, Michigan, 2011.
- Castro, JTP, Meggiolaro, MA., *Fadiga – Técnicas e Práticas de Dimensionamento Estrutural sob Cargas Reais de Serviço*, Lexington, 2009.

CONTACT INFORMATION

ademar@gacsolucoes.com.br / silvio@altair.com

ABBREVIATIONS

- ε_1 – notch major principal strain;
- ε_2 – notch minimum principal strain;
- ε_3 – notch surface normal strain;
- ε_{eq} – notch equivalent strain;
- ε_a – total amplitude strain;
- σ_1 – notch major principal stress;
- σ_2 – notch minimum principal stress;
- σ_3 – notch surface normal stress;

σ_{eq} – notch equivalent stress;

${}^e\sigma_1$ – elastic major stress;

${}^e\sigma_2$ – elastic minimum stress;

${}^e\sigma_3$ – elastic surface normal stress;

${}^e\sigma_{eq}$ – elastic equivalent stress;

${}^e\varepsilon_1$ – elastic major strain;

${}^e\varepsilon_2$ – elastic minimum strain;

${}^e\varepsilon_3$ – elastic surface normal strain;

${}^e\varepsilon_{eq}$ – elastic equivalent strain;

E – modulus of elasticity.

E^* – effective modulus of elasticity.

n – monotonic strength exponent.

H – monotonic strength coefficient.

H^* – effective strength coefficient.

ε'_f – fatigue ductility coefficient.

c – fatigue ductility exponent.

σ'_f – fatigue strength coefficient.

b – fatigue strength exponent.

$2N_f$ – number de reversals to failure.

ν – Poison ratio.

$\bar{\nu}$ – effective Poison ratio.